Selective CO_2 sorption using a compartmentalized coordination polymer with discrete voids

Eugenia Miguel-Casañ,[a] Eduardo Andres-Garcia,[a] Joaquin Calbo,[a] Mónica Giménez-Marqués[a] and Guillermo Mínguez Espallargas*[a]

We report a novel Fe(II) compartmentalized coordination polymer (CCP) capable of physisorbing gas molecules in a selective manner. The crystal structure was modelled theoretically under the Density Functional Theory revealing the presence of discrete voids of 380 Å^3, significantly larger than those reported for its predecesors. Adsorption isotherms of pure N_2, CH_4 and CO_2 were measured, obtaining a loading capacity of 0.6, 1.7 and 2.2 molecules/void at 10 bar and at 298 K. Dynamic breakthrough gas experiments have been performed at different fluxes and temperatures, showing efficient adsorption and excellent selectivities for CO_2 in gas mixtures with methane and nitrogen.

Introduction

Carbon dioxide (CO_2) is the single most important anthropogenic greenhouse gas in the atmosphere, with a global average increase from 278 to 405 ppm in the last 30 years.[1] Therefore, the quest for carbon capture materials has moved to the forefront of scientific research in order to slow down this increasing concentration of CO_2 level in the atmosphere.[2]

Currently, the common technique to absorb CO_2 on post-combustion capture are aqueous amines scrubbers.[3] However, the exorbitant energy consumption and the corrosion issues directly derived from this process entail many disadvantages, and promote the success opportunities for other materials.[4] Possible solutions include cryogenic distillation, that implies higher energy; membranes, that are mechanically fragile; and, microbial/algae capture materials, with an extremely narrow operation conditions range.[5] Although each of them can also provide excellent results, adsorption processes are better alternatives as both operational energy and costs are reduced. The use of porous materials, such as zeolites,[6] activated carbons,[7] or porous coordination polymers (CPs, also known as metal-organic frameworks, or MOFs),[8] has been adequately considered due to the frequent weak interactions between the sorbate and sorbent,[9] resulting in the advantageous reduced cost of the regenerability of the material.[10]

Porous CPs, with more than 70.000 reported compounds,[11] have an ample variety of structures, some of them with channels of appropriate reduced sizes to allocate exclusively CO_2 molecules, which are slightly smaller than N_2. In addition, the large chemical versatility of these CPs allows to modify the framework inner space to incorporate different functionalities and promote specific interactions.[12,13] In this sense, the introduction of specific binding sites for CO_2 to interact, including open-metal sites[14] or Lewis basic sites,[15] has been demonstrated as an efficient solution to separate CO_2 from mixtures of gases.[16,17]

An alternative approach consists on the use of discrete compartments, where the gas molecules are confined in a restricted space, but without establishing a strong interaction with the framework. These compartmentalized coordination polymers (CCPs) lack permanent channels for gas diffusion occurring as in traditional porous materials, but nevertheless small molecules can diffuse inside the voids thanks to the dynamic rotation of the organic ligands.[18] We have previously reported a family of CCPs which are composed of two tetrazole groups that coordinate to Fe^{II}, resulting in 1D coordination polymers in which the metal centers are triply bridged by the organic ligands.[19] This family of materials possesses internal cavities that have been proved suitable for the allocation of gas molecules. Specifically, the use of the ligand 1,4-bis(tetrazol-1-ylmethyl)benzene yields **CCP-1** and **CCP-2** (respectively with ClO_4^- or BF_4^- as counterions), two compartmentalized coordination polymers that can incorporate one molecule of gas per void. In addition, the use of discrete compartments was shown to be very efficient for the separation of CO_2 from industrial mixtures of CO_2/N_2 and CO_2/CH_4.[20]

Herein, we expand our previous work on the use of CCPs for gas separation with the chemical design of a novel ligand that expands the size of the internal void. Specifically, 4,4''-bis((1H-tetrazol-1-yl)methyl)-1,1':4',1''-terphenyl, hereafter btztp, has an increased distance between the coordinating tetrazole rings of 18.3 Å (see Scheme 1), which should permit the formation of new CCPs with larger voids capable of incorporating a larger amount of gas molecules. In addition, as the mechanism of sorption is expected to be similar to the previously reported for CCPs, we hypothesised that the increase in CO_2 sorption should be accompanied with a negligible N_2 sorption, thus resulting in an enhanced separation capacity.

Results and discussion

Crystal structure and characterization

In order to obtain large cavities with the aim of increasing the sorption capacity of compartmentalized coordination polymers, the ligand btztp was designed based on the previously reported ligands btzx and btzbp (see Scheme 1). These have been used for the preparation of **CCP-1** and **CCP-2** (btzx),[19,20] and **CCP-3** and **CCP-4** (btzbp).[21] The ligand btztp was prepared adapting a previously reported protocol for the formation of tetrazole,[22] consisting on the reaction of terphenyl-bis-amine with NaN_3 and triethylorthoformate (see Supporting Information). The first step consisted in the formation of the terphenyl-bis-amine molecule via a Suzuki coupling between 4-bromobenzylamine and benzene-1,4-diboronic acid, after protecting the amine groups and the boronic acids (see Supporting Information).
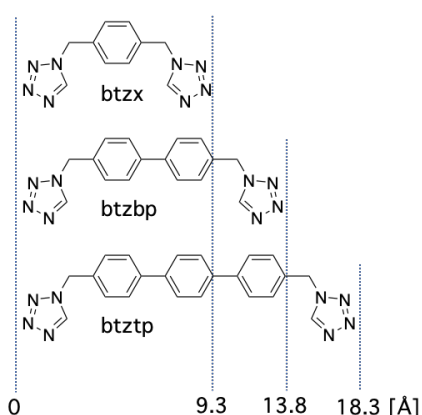
Scheme 1. Chemical structures of the different ligands btzx (top), btzbp (middle) and btztp (bottom), used for the formation of **CCP-1** and **CCP-2** (top), **CCP-3** and **CCP-4** (middle) and **CCP-5** and **CCP-6** (bottom). **CCP-1**, **CCP-3** and **CCP-5** possess ClO_4^- as counterions, whereas **CCP-2**, **CCP-4** and **CCP-6** have BF_4^- as counterion. The dashed arrows represent the distances between the two coordinating nitrogens.

The reaction of btztp with two different Fe(II) salts in refluxing MeCN for 5 days affords two coordination polymers, denoted **CCP-5** and **CCP-6**, with the general formula $[Fe(btztp)_3](X)_2$ (X = ClO_4 or BF_4, respectively). These crystalline materials were characterized by XRPD, EDAX, IR, TGA and magnetic measurements (see Supporting Information), which all confirm the chemical composition of the materials. Essentially, the presence of spin-crossover phenomena confirms that each Fe(II) centre is coordinated by 6 tetrazoles, resulting in a coordination environment analogous to the previously reported Fe(II) coordination polymers based on similar bistetrazole ligands.[19–21, 23]

Both **CCP-5** and **CCP-6** show a gradual and incomplete spin transition with the transition temperature centred at 204 K (see Figure S5). Unfortunately, despite countless efforts dedicated to obtaining crystals large enough for single crystal diffraction, structure determination has been unsuccessful. To circumvent this issue, we have been able to model **CCP-6** and obtain its crystal structure under the Density Functional Theory (see Experimental for full computational details). The initial geometry of **CCP-6** at the low-spin state was modelled taking into account previous single crystal diffraction data obtained from **CCP-2** and **CCP-4**, and then the atomic positions and cell parameters were optimized at the PBEsol level including BF_4^- counterions for charge neutrality (Figure 1). Coordination Fe^{II}–N distances are predicted at 1.93 Å, similar to crystal structures of **CCP-2** and **CCP-4** calculated at the same level, and in good accord with previous experimental data.[20,21] Importantly, the pore size in **CCP-6** is significantly increased, with a Fe center-to-center distance of 19.9 Å, with respect to **CCP-2** (11.4 Å) and **CCP-4** (15.7 Å). As shown in Figure 2, the calculated powder pattern of this model is in good agreement with the experimental powder pattern.
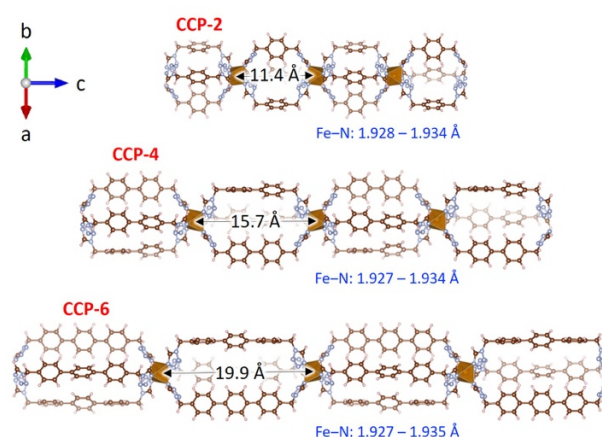

Figure 1. Minimum-energy crystal structure of **CCP-2**, **CCP-4** and **CCP-6** calculated at the PBEsol level of theory. Coordination Fe^{II}–N distances are indicated in blue. BF_4^- counterions are omitted for clarity.

Structural analysis confirms the formation of 1D chains in which the metal centres are triply bridged by btztp ligands, which coordinate in a *syn*-conformation. The distance between adjacent Fe centers (19.9 Å) is larger than the typically observed for cooperative spin-crossover phenomena, which agrees with the gradual thermal transition observed in the magnetic measurements. The arrangement of the ligand causes the formation of discrete voids with a volume of *ca*. 380 Å^3, significantly larger than those found in **CCP-1** and **CCP-2** (135 Å^3), and **CCP-3** and **CCP-4** (253 Å^3). Each of these voids is partially occupied by MeCN molecules, as deduced from TGA measurements (see Figure S7), but these molecules can be easily evacuated upon simple activation protocol.
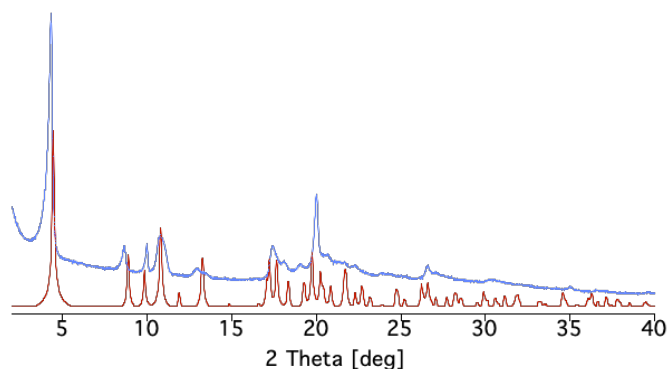
Figure 2. Experimental (blue) and calculated (red) X-ray powder diffractograms of **CCP-6**.
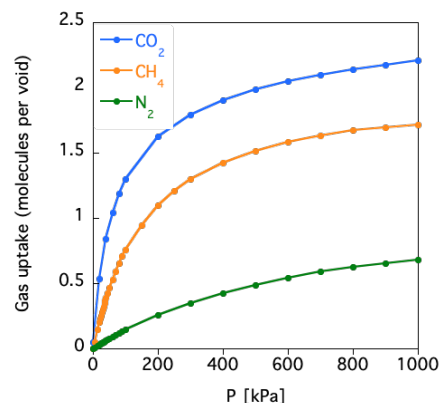

Figure 3. CO_2, N_2 and CH_4 gas adsorption isotherms of **CCP-6** at 298 K. Equilibrium conditions set to 600 s intervals, with a tolerance of 0.001 mg min^{-1}.

Single-component CO_2, CH_4 and N_2 adsorption

CCPs have demonstrated the capacity of loading different gases in their internal voids, even though the crystal structures present no permanent channels.[20] Analysis of the sorption capability of activated **CCP-6** towards N_2, CH_4 and CO_2 (Figure 3) has been therefore conducted. Due to the isostructurality of **CCP-5** and **CCP-6**, a similar sorption capacity is expected in these two materials, as was observed for **CCP-1** and **CCP-2**.[20]

Figure 3 depicts the obtained experimental sorption isotherms for N_2, CH_4 and CO_2 at 298 K, respectively obtaining a loading capacity of 0.6, 1.7 and 2.2 molecules/void at 10 bar. As expected, the gas capacity of **CCP-6** has been increased with respect to the analogues **CCP-1** − **CCP-4** obtained with the shorter bis-tetrazole ligands. These results, and the shapes of the curves, suggest a likely ability to separate those gases from mixtures (*vide infra*). A characteristic thermodynamic sorption behaviour occurs for CO_2 and CH_4 sorption at different temperatures (283, 298, 313 and 333 K), with the corresponding sorption capacity increase at lower temperatures (Figure S9). The isotherms for both gases describe an abrupt and sharp profile (especially for the carbon dioxide branch) with no evident hysteresis observed. The adsorption affinity for CO_2 has been quantified using the calculated isosteric heat of adsorption (Q_{st}) from the Clausius-Clapeyron equation using the adsorption data collected. The isosteric heat of adsorption for CO_2 at zero coverage on **CCP-6** was estimated to be 29 kJ mol^{-1} (see Figure S11), which is slightly higher than that found in **CCP-4** (16.3 kJ mol^{-1}) and **CCP-2** (22.0 kJ mol^{-1}).

Even though all the three gas molecules can physically fit in the void, as the kinetic diameters of CO_2, N_2 and CH_4 are different (3.3, 3.64 and 3.8 Å, respectively), the lack of permanent channels enhances the role of the interaction between the gases and the framework for gas sorption. Analysis of the adsorption kinetic profiles for CO_2, CH_4 and N_2, indicates that CO_2 gas possesses the lowest threshold pressure as compared with CH_4 and N_2 (Figure S12). Furthermore, CO_2 desorption occurs under longer times, likely due to its higher

affinity with the **CCP-6** framework. These two observations arising from single-gas sorption point to a preferential adsorption of CO_2 gas over CH_4 or N_2, which have been further investigated in real mixtures using breakthrough measurements.

Breakthrough: CO_2/CH_4 and CO_2/N_2 separations

Breakthrough measurements are useful to study the real capacity of a material to separate a given gas from a mixture. Essentially, we have investigated the capacity of **CCP-6** to separate CO_2 from CO_2:N_2 and CO_2:CH_4 mixtures, which is a relevant process in industrial applications, as CO_2 is an anthropogenic pollutant and methane is a highly demanded fuel. For this, CO_2 has been diluted in three ratios, namely 1:1, 1:3 and 1:5 (CO_2:N_2/CH_4), maintaining the final pressure at 1 bar and adding helium as a system tracer. Note that the use of the helium tracer in the breakthrough experiments allows also to ensure a negligible adsorption of both nitrogen and methane. In addition, the role of the temperature in the separation capacity of this compartmentalized polymer has been also investigated in the 1:3 dilution using three different temperatures, namely 283, 298 and 323 K.

Figure 4 displays the summary of the experimental results, comparing the adsorption of the different gases in each mixture at diverse operation conditions (see Figures S13-S17 for breakthrough profiles). A similar behavior is found for CO_2:N_2 and CO_2:CH_4 mixtures , resulting in **CCP-6** being capable to fully extract CO_2 from these mixtures reaching excellent purity, especially at high CO_2 concentration. Nitrogen and methane are both negligibly adsorbed in most of the situations. As already reported, an increase in the concentration of carbon dioxide can lead to an additional contribution to the electrostatic interactions, thus favouring CO_2 selectivities.[24] This CO_2 selectivity is also enhanced at lower temperatures, corresponding to the thermodynamic behavior of an exothermal adsorption.
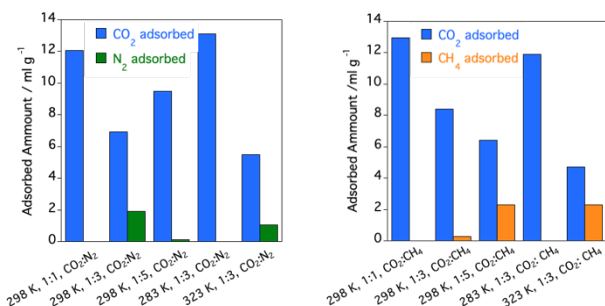
Figure 4. Gas adsorbed amounts on **CCP-6** determined from breakthrough profiles, at 1 bar (absolute pressure) for $CO_2:N_2$ (left) and $CO_2:CH_4$ (right) mixtures at different ratios (1:1, 1:5 and 1:3) and different temperatures 283, 298 and 323 K. Time zero is set with the first detection of helium (tracer).

Table 1 displays the experimental results from the breakthrough measurements, indicating the dynamic selectivity value (α), calculated through the adsorbed amounts and the inlet concentrations (see Section S5 in the Supporting Information). An α value larger than 1 means that the material is capable of selectively adsorb CO_2 from the mixtures, and serves to compare the efficiency of different materials. As can be seen, the $CO_2:N_2$ and $CO_2:CH_4$ separations are more efficient at higher CO_2 concentrations (and lower fluxes) and at lower temperatures.

Table 1. Experimental selectivities (α) for **CCP-6**, calculated from the integration of the respective breakthrough curves. CO_2 is kept constant, and diluted in nitrogen to achieve different composition ratios.

	1:1 ($CO_2:N_2$)	1:3 ($CO_2:N_2$)	1:5 ($CO_2:N_2$)
283 K		>1000	
298 K	>1000	294	17
323 K		15	

	1:1 ($CO_2:CH_4$)	1:3 ($CO_2:CH_4$)	1:5 ($CO_2:CH_4$)
283 K		>1000	
298 K	>1000	88	14
323 K		6	

Despite the limited amount of CO_2 sorbed by **CCP-6** in the breakthrough experiments (0.22-0.58 mmol·g^{-1}) as compared with traditional porous materials (range: 0.15-3.75 mmol·g^{-1}), particularly large experimental selectivities (α) are observed as a consequence of a remarkably negligible sorption of N_2 or CH_4 when CO_2 is present. Such excellent selectivities place **CCP-6** among the best PCPs/MOFs for these separations (see Table 2). Regeneration is successfully achieved at mild conditions, thus resulting in a remarkable separation efficiency. Specifically, **CCP-6** is regenerated at room temperature, without the necessity of heating. It should be emphasized that temperature is one of most critical parameter, as an increase in energy consumption will affect the viability of industrial efficiency. Although **CCP-6** is not the only MOF regenerated at ambient

temperature,[25,26] most of their competitors require 100-200 °C, specially once methane is part of the target mixture.[27,28,29,30,31]

Table 2. Experimental selectivities (α) extracted from breakthrough measurements from selected MOFs.

1:1 ($CO_2:N_2$)	T / P	α	Ref.
CCP-6	298 K / 1 bar	>1000	This work
CCP-1	298 K / 2 bar	2	20
MIL-100(Fe)	303 K	8.6	32
MIL-53(Al)-NH_2	303 K / 1 bar	<75	33
MOF-508b	303 K	5	34
ZIF-95	RT	18	26
ZIF-100	RT	25	26

1:1 ($CO_2:CH_4$)	T / P	α	Ref.
CCP-6	298 K / 1 bar	>1000	This work
CCP-1	298 K / 2 bar	2	20
CPO-27 (Ni)	303 K / 1 bar	15	35
CPO-27 (Co)	303 K / 1 bar	12	35
CPO-27 (Zn)	303 K / 1 bar	9	35
Cu-BTC)	303 K / 1 bar	6.6	27
MIL-100(Fe)	303 K	5.3	32
MIL-101(Al)-NH_2	298 K / 1 bar	6.3	28
MIL-53(Al)-NH_2	303 K / 1 bar	45	30

Conclusions

In summary, we have designed a new compartmentalized coordination polymer that selectively separates CO_2 from different gas mixtures. The new compartmentalized coordination polymer, of formula [Fe(btztp)$_3$](X)$_2$ (X = ClO_4 or BF_4), denoted **CCP-5** and **CCP-6**, respectively, contains large discrete cavities of 380 Å^3, suitable to allocate a larger amount of CO_2 gas molecules than the previously reported CCPs. The selective sorption capacity of **CCP-6** has been experimentally demonstrated with breakthrough experiments, resulting in excellent selectivity values, thus being competitive with some molecular sieving zeolites, such as RHO.[34] The high selectivity of **CCP-6** at high CO_2 concentration and its facile regenerability denote that **CCP-6** could find applicability in industrial processes involving the purification of highly contaminated streams, or as a first step in a multiple-stage process. Finally, this facile regenerability of the material, which allows subsequent uses, facilitates its implementation in chemical engineering industry.

Experimental

Materials and methods

All chemicals used were purchased from commercial sources and used without further purification, unless specially mentioned. Anhydrous dichloromethane, acetonitrile, and tetrahydrofuran solvents were freshly distilled under argon over the appropriate drying agent (calcium chloride, calcium hydroxide and sodium, respectively). Column chromatography was carried out on silica gel (60 Å, 230–400 mesh).

^{1}H NMR spectra were acquired on a Bruker AVANCE DRX 300 spectrometer. The spectra were referred to residual proton-solvent references.

High-resolution (MALDI-TOF/TOF) mass spectra were recorded in a 5800 MALDI TOF/TOF (ABSciex) in positive reflector mode.

Synthesis of [Fe(btztp)$_3$](X)$_2$ (X = ClO$_4$ or BF$_4$) (CCP-5 and CCP-6). A solution of Fe(ClO$_4$)$_2$·xH$_2$O (12 mg, 0.03 mmol) (for **CCP-5**) or Fe(BF$_4$)$_2$·xH$_2$O (12 mg, 0.03 mmol) (for **CCP-6**) in 6 mL of MeCN was added into a suspension of **btztp** (20 mg, 0.05 mmol) in 6 mL of MeCN. A white crystalline precipitate appeared after a few days. The white powder was filtered and washed with MeCN. Phase purity was established by X-ray powder diffraction (vide infra). Yield 70% for **CCP-5** and 75% for **CCP-6**.

Calculations. The minimum-energy geometry of **CCP-2**, **CCP-4** and **CCP-6** were obtained upon full ion and lattice relaxation under periodic boundary conditions using the FHI-AIMS program package.[36,37,38] The initial geometry of **CCP-6** was extracted from the X-ray crystal of parent **CCP-2** and **CCP-4**. BF$_4^-$ counterions were added for charge neutrality. The unit cell for **CCP-2**, **CCP-4** and **CCP-6** contained 190, 250 and 310 atoms in total, respectively, and the low-spin state was calculated in all cases. The revised semi-local Perdew-Burke-Ernzerhof GGA PBEsol functional was used throughout. The recommended level of scalar relativity "atomic ZORA" approximation in FHI-AIMS was employed according to Ref. [39]. The following convergence criteria for the self-consistency cycle were applied: charge density 1E-4, sum of eigenvalues 1E-2, and total energy 1E-5. For the geometry relaxation, the trust radius method enhanced version of the Broyden-Fletcher-Goldfarb-Shanno (BFGS) optimization algorithm was employed,[40] with an energy tolerance of 1E-3 and a maximum residual force component per atom of 1E-2. All lattice vector degrees of freedom were relaxed. The minimum-energy structure calculated for **CCP-2/4/6** are shown in Figure 1. Optimized lattice parameters are summarized in Table S1.

X-ray powder diffraction. Polycrystalline samples of **CCP-5** and **CCP-6** were lightly ground in an agate mortar and pestle and filled into 0.5 mm borosilicate capillaries prior to being mounted and aligned on an Empyrean PANalytical powder diffractometer, using Cu Kα radiation (λ = 1.54056 Å). For each sample, two repeated measurements were collected at room temperature (2θ = 2-60°) and merged into a single diffractogram.

Magnetic measurements. Magnetic susceptibility measurements were carried out on single-phase polycrystalline samples with a Quantum Design MPMS-XL-5 SQUID susceptometer. The susceptibility data were all collected at 1 K·min^{-1}, with an applied field of 0.1 T. Magnetic susceptibility measurements of the gas loaded systems were performed by sealing a glass tube with 10 mg of CCP-6 and a known amount of CO$_2$ molecules. Prior to the gas loading, the samples were activated by heating in situ at 150 °C for 3 h under vacuum. In order to discard leak effects, the experiment was repeated twice obtaining the same results.

Gas sorption isotherms. High-pressure adsorption isotherms of CO$_2$, CH$_4$ and N$_2$ were measured at different temperatures ranging from 283 to 333 K in an IGA-001 gravimetric single component gas sorption analyser (Hiden Isochema) using approximately 50 mg of sample. Before each adsorption experiment, the sample was outgassed at 423 K under a vacuum (10^{-5} Pa) for two hours. The sample was then cooled down, still under high vacuum, to the target temperature that was controlled using a recirculating thermostatic bath. Equilibrium conditions corresponded to 600 s. interval, and 0.001 mg·min^{-1} tolerance. Virial equations were applied for fitting experimental data points with a fourth-grade polynomial used to properly describe the CO$_2$ isotherms. The heat of adsorption was calculated according to the Clausius-Clapeyron equation through the data extracted from the experimental isotherms at different temperatures.

Breakthrough setup. An ABR (HIDEN Isochema) automated breakthrough analyzer setup based on a packed adsorption column was used to determine the adsorption dynamics of pure gases and mixtures. Pressure, temperature and inlet composition can be controlled and tuned for each experiment, and the outlet composition is analysed by an integrated mass spectrometer (HPR-20 QIC). The fixed-bed column was filled with 341 mg of CCP-6. Before each measurement, the sample was regenerated at atmospheric temperature and pressure, in 40 mL·min^{-1} Ar flow for 20 minutes. Operation conditions ranged 283-323 K at 1 bar. The inlet mixture consisted of carbon dioxide diluted in N$_2$ or CH$_4$ (1:1, 3:1, 5:1; CO$_2$:N$_2$/CH$_4$). Time zero was set with the first detection of helium, which was used as a trace (2 mL·min^{-1} of He in the feed flow).

Conflicts of interest

There are no conflicts to declare.

Acknowledgements

References

1   World Meteorological Organization and Atmosphere Watch Global, *World Meteorol. Organ. Bull.*, 2017, 1–4.

2   M. Oschatz and M. Antonietti, *Energy Environ. Sci.*, 2018, **11**, 57–70.

3   G. T. Rochelle, *Science*, 2009, **325**, 1652–1654.

4   K. Sumida, D. L. Rogow, J. A. Mason, T. M. McDonald, E. D. Bloch, Z. R. Herm, T. H. Bae and J. R. Long, *Chem. Rev.*, 2012, **112**, 724–781.

5   J. R. Li, Y. Ma, M. C. McCarthy, J. Sculley, J. Yu, H. K. Jeong, P. B. Balbuena and H. C. Zhou, *Coord. Chem. Rev.*, 2011, **255**, 1791–1823.

6   R. V. Siriwardane, M. S. Shen, E. P. Fisher and J. Losch,

Energy and Fuels, 2005, **19**, 1153–1159.

7   R. V. Siriwardane, M. S. Shen, E. P. Fisher and J. A. Poston, *Energy and Fuels*, 2001, **15**, 279–284.

8   Y. Belmabkhout, V. Guillerm and M. Eddaoudi, *Chem. Eng. J.*, 2016, **296**, 386–397.

9   A. Kumar, D. G. Madden, M. Lusi, K. J. Chen, E. A. Daniels, T. Curtin, J. J. Perry and M. J. Zaworotko, *Angew. Chemie - Int. Ed.*, 2015, **54**, 14372–14377.

10   M. Songolzadeh, M. T. Ravanchi and M. Soleimani, 2012, **6**, 900–907.

11   P. Z. Moghadam, A. Li, S. B. Wiggin, A. Tao, A. G. P. Maloney, P. A. Wood, S. C. Ward and D. Fairen-Jimenez, *Chem. Mater.*, 2017, **29**, 2618–2625.

12   O. Shekhah, Y. Belmabkhout, Z. Chen, V. Guillerm, A. Cairns, K. Adil and M. Eddaoudi, *Nat. Commun.*, 2014, **5**, 4228.

13   S. Yang, A. J. Ramirez-Cuesta, R. Newby, V. Garcia-Sakai, P. Manuel, S. K. Callear, S. I. Campbell, C. C. Tang and M. Schröder, *Nat. Chem.*, 2015, **7**, 121–129.

14   B. Chen, M. Eddaoudi, T. M. Reineke, J. W. Kampf, M. O'Keeffe and O. M. Yaghi, *J. Am. Chem. Soc.*, 2000, **122**, 11559–11560.

15   S. Couck, J. F. M. Denayer, G. V. Baron, T. Rémy, J. Gascon and F. Kapteijn, *J. Am. Chem. Soc.*, 2009, **131**, 6326–6327.

16   Y. Ye, H. Zhang, L. Chen, S. Chen, Q. Lin, F. Wei, Z. Zhang and S. Xiang, *Inorg. Chem.*, 2019, **58**, 7754–7759.

17   M. Asgari, S. Jawahery, E. D. Bloch, M. R. Hudson, R. Flacau, B. Vlaisavljevich, J. R. Long, C. M. Brown and W. L. Queen, *Chem. Sci.*, 2018, **9**, 4579–4588.

18   T. Jacobs, G. O. Lloyd, J.-A. Gertenbach, K. K. Müller-Nedebock, C. Esterhuysen and L. J. Barbour, *Angew. Chemie Int. Ed.*, 2012, **51**, 4913–4916.

19   E. Coronado, M. Giménez-Marqués, G. Mínguez Espallargas, F. Rey and I. J. Vitórica-Yrezábal, *J. Am. Chem. Soc.*, 2013, **135**, 15986–15989.

20   M. Giménez-Marqués, N. Calvo Galve, M. Palomino, S. Valencia, F. Rey, G. Sastre, I. J. Vitórica-Yrezábal, M. Jiménez-Ruiz, J. A. Rodríguez-Velamazán, M. A. González, J. L. Jordá, E. Coronado and G. Mínguez Espallargas, *Chem. Sci.*, 2017, **8**, 3109–3120.

21   N. Calvo Galve, M. Giménez-Marqués, M. Palomino, S. Valencia, F. Rey, G. Mínguez Espallargas and E. Coronado, *Inorg. Chem. Front.*, 2016, **3**, 808–813.

22   P. N. Gaponik, V. P. Karavai and Y. V. Grigor'ev, *Chem. Heterocycl. Compd.*, 1985, **21**, 1255–1258.

23   M. Quesada, F. Prins, E. Bill, H. Kooijman, P. Gamez, O. Roubeau, A. L. Spek, J. G. Haasnoot and J. Reedijk, *Chem. - A Eur. J.*, 2008, **14**, 8486–8499.

24   J. R. Karra and K. S. Walton, *J. Phys. Chem. C*, 2010, **114**, 15735–15740.

25   V. Finsy, L. Ma, L. Alaerts, D. E. De Vos, G. V. Baron and J. F. M. Denayer, *Microporous Mesoporous Mater.*, 2009, **120**, 221–227.

26   B. Wang, A. P. Côté, H. Furukawa, M. O'Keeffe and O. M. Yaghi, *Nature*, 2008, **453**, 207–211.

27   L. Hamon, P. L. Llewellyn, T. Devic, A. Ghoufi, G. Clet, V. Guillerm, G. D. Pirngruber, G. Maurin, C. Serre, G. Driver,

W. van Beek, E. Jolimaître, A. Vimont, M. Daturi and G. Férey, *J. Am. Chem. Soc.*, 2009, **131**, 17490–17499.

28   P. Serra-Crespo, E. V. Ramos-Fernandez, J. Gascon and F. Kapteijn, *Chem. Mater.*, 2011, **23**, 2565–2572.

29   R. L. Siegelman, P. J. Milner, A. C. Forse, J.-H. Lee, K. A. Colwell, J. B. Neaton, J. A. Reimer, S. C. Weston and J. R. Long, *J. Am. Chem. Soc.*, 2019, **141**, 13171–13186.

30   S. Couck, E. Gobechiya, C. E. A. Kirschhock, P. Serra-Crespo, J. Juan-Alcañiz, A. Martinez Joaristi, E. Stavitski, J. Gascon, F. Kapteijn, G. V. Baron and J. F. M. Denayer, *ChemSusChem*, 2012, **5**, 740–750.

31   L. Bastin, P. S. Bárcia, E. J. Hurtado, J. A. C. Silva, A. E. Rodrigues and B. Chen, *J. Phys. Chem. C*, 2008, **112**, 1575–1581.

32   S. Xian, J. Peng, Z. Zhang, Q. Xia, H. Wang and Z. Li, *Chem. Eng. J.*, 2015, **270**, 385–392.

33   E. Stavitski, E. A. Pidko, S. Couck, T. Remy, E. J. M. Hensen, B. M. Weckhuysen, J. Denayer, J. Gascon and F. Kapteijn, *Langmuir*, 2011, **27**, 3970–3976.

34   M. Palomino, A. Corma, J. L. Jordá, F. Rey and S. Valencia, *Chem. Commun.*, 2012, **48**, 215–217.

35   J. Liu, J. Tian, P. K. Thallapally and B. P. McGrail, *J. Phys. Chem. C*, 2012, **116**, 9575–9581.

36   H. Shang, N. Raimbault, P. Rinke, M. Scheffler, M. Rossi and C. Carbogno, *New J. Phys.*, 2018, **20**, 073040.

37   V. Havu, V. Blum, P. Havu and M. Scheffler, *J. Comput. Phys.*, 2009, **228**, 8367–8379.

38   V. Blum, R. Gehrke, F. Hanke, P. Havu, V. Havu, X. Ren, K. Reuter and M. Scheffler, *Comput. Phys. Commun.*, 2009, **180**, 2175–2196.

39   J. P. Perdew, A. Ruzsinszky, G. I. Csonka, O. A. Vydrov, G. E. Scuseria, L. A. Constantin, X. Zhou and K. Burke, *Phys. Rev. Lett.*, 2008, **100**, 136406.

40   J. Nocedal and S. J. Wright, *Numerical Optimization*, 2006, vol. 2nd Edition.